Harmful Algae 110 (2021) 102117

Contents lists available at ScienceDirect

Harmful Algae

journal homepage: www.elsevier.com/locate/hal

Original article

Stable isotope analysis reveals differences in domoic acid accumulation and feeding strategies of key vectors in a California hotspot for outbreaks

Sophie Bernstein [a], Rocio I. Ruiz-Cooley [a,b,*], Raphael Kudela [c], Clarissa R. Anderson [d], Robin Dunkin [c], John C. Field [e]

[a] Moss Landing Marine Laboratories, 8272 Moss Landing Road, Moss Landing, CA 95039, USA
[b] Departamento de Oceanografía Biológica, Centro de Investigación Científica y de Educación Superior de Ensenada (CICESE), Ensenada, México
[c] University of California-Santa Cruz, 1156 High Street, Santa Cruz, CA 95064, USA
[d] Scripps Institution of Oceanography/Southern California Coastal Ocean Observing System, University of California, San Diego, Scripps Institute of Oceanography, 8880 Biological Grade La Jolla, CA 92037, USA
[e] National Oceanic and Atmospheric Administration, Fisheries Ecology Division, Southwest Fisheries Science Center 110 McAllister Way Road Santa Cruz, CA 95060, USA

ARTICLE INFO

Keywords:
Stable isotopes
California current system
Monterey Bay
Harmful algal bloom
Trophic transfer
Pseudo-nitzschia

ABSTRACT

Given the effects of harmful algal blooms (HABs) on human and wildlife health, understanding how domoic acid (DA) is accumulated and transferred through food webs is critical for recognizing the most affected marine communities and predicting ecosystem effects. This study combines stable isotopes of carbon ($\delta^{13}C$) and nitrogen ($\delta^{15}N$) from bulk muscle tissue with DA measurements from viscera to identify the foraging strategies of important DA vectors and predators in Monterey Bay, CA. Tissue samples were collected from 27 species across three habitats in the summer of 2018 and 2019 (time periods without prominent HABs). Our results highlight an inshore-offshore variation in krill $\delta^{13}C$ values and DA concentrations ([DA]; ppm) in anchovies indicating differences in coastal productivity and DA accumulation. The narrow overlapping isotopic niches between anchovies and sardines suggest similar diets and trophic positions, but striking differences in [DA] indicate a degree of specialization, thus, resource partitioning. In contrast, krill, market squid, and juvenile rockfish accumulated minimal DA and had comparatively broad isotopic niches, suggesting a lower capacity to serve as vectors because of potential differences in diet or feeding in isotopically distinct locations. Low [DA] in the liver of stranded sea lions and their generalist foraging tendencies limits our ability to use them as sentinels for DA outbreaks in a specific geographic area. Collectively, our results show that DA was produced a few kilometers from the coastline, and anchovies were the most powerful DA vector in coastal-pelagic zones (their DA loads exceeded the 20 ppm FDA regulatory limits for human consumption), while mussels did not contain detectable DA and only reflect in situ DA, $\delta^{13}C$, and $\delta^{15}N$ values. Our study demonstrates the efficacy of combining multiple biogeochemical tracers to improve HAB monitoring efforts and identify the main routes of DA transfer across habitats and trophic levels.

1. Introduction

Harmful Algal Blooms (HABs) are increasing in frequency, intensity, and geographic range, threatening open ocean and coastal ecosystems worldwide (Bates et al., 2018). In the California Current System (CCS), HABs have been documented nearly every year since 1991, concurrent with anthropogenic stressors that alter phytoplankton assemblages (Sun et al., 2011; Lewitus et al., 2012; Trainer et al., 2020). Many of these HABs are associated with domoic acid (DA), a toxin produced by *Pseudo-nitzschia* spp., including the prolific toxin-producers, *Pseudo-nitzschia multiseries* and *Pseudo-nitzschia australis* (Horner et al., 1997; Trainer et al., 2000). When ingested by humans, DA can cause the potentially fatal Amnesic Shellfish Poisoning (Bates et al., 1989). As a result, commercial and recreational shellfish and finfish fisheries, including Dungeness crab (*Metacarcinus magister*), anchovy (*Engraulis mordax*), and sardine (*Sardinops sagax*), are closely monitored to protect human health (Lewitus et al., 2012; Anderson et al., 2019). These fisheries are particularly susceptible to seasonal closures in response to DA

* Corresponding author.
E-mail addresses: sophiebernstein94@gmail.com (S. Bernstein), ruizrc@cicese.mx (R.I. Ruiz-Cooley).

https://doi.org/10.1016/j.hal.2021.102117
Received 29 April 2021; Received in revised form 20 September 2021; Accepted 22 September 2021
Available online 25 October 2021

outbreaks, often resulting in economic hardship for coastal communities (McCabe et al., 2016; Ritzman et al., 2018; Holland and Leonard, 2020). DA episodes are also responsible for mass morbidity and mortality of marine mammals and seabirds, thereby threatening ecosystem balance (Work et al., 1993; Scholin et al., 2000). Yet, detailed, comparative explanations on the role that foraging strategies play in explaining the capacity for a given species to serve as a DA vector have not been provided, and, as a result, detecting the onset of a toxic event is often delayed. These topics are addressed in the current study.

The widespread ecosystem consequences of DA events call for abundant monitoring and forecasting initiatives, which are limited in capacity because of challenges of acquiring data from non-coastal regions. Phytoplankton composition and water quality are measured weekly at nine coastal sites in California (Anderson et al., 2019). DA concentrations from mussels are also measured routinely at the Santa Cruz Wharf (SCW). DA concentrations in mussels align well with particulate DA (pDA) concentrations from phytoplankton in the water, making mussels reliable indicators of DA accumulation in primary consumers and toxin presence along the coastline (Lane et al., 2009; Anderson et al., 2016); however, these routine efforts only detect HABs within ~4 km from the shoreline (Kudela et al., 2012; Frolov et al., 2013). In the pelagic zone, the precise locations of bloom initiation and DA production are not clearly identified because the oceanographic conditions favoring such blooms are spatially and temporally variable, and not all *Pseudo-nitzschia* spp. produce toxins (Ryan et al., 2014; Bowers et al., 2018). The species composition of toxin-producing phytoplankton communities determines the level of DA content and the DA content is highly influenced by temperature, micro- and macro-nutrient concentrations and wind-driven upwelling, among other factors, which vary in space and time (Trainer et al., 2020). This was evident during 2015 when *Pseudo-nitzschia* blooms were initiated by anomalously warm ocean conditions and biophysical changes: in Monterey Bay, blooms became toxic after upwelling removed warm waters and shifted ambient nutrient ratios (Ryan et al., 2017). DA production along coastal Oregon and Washington was driven mainly by spring storms delivering blooms from offshore waters (McCabe et al., 2016). The spatial and temporal complexity surrounding DA production makes it difficult to predict the primary routes of DA trophic transfer.

The routes of DA transfer and exposure to consumers are difficult to determine given that being an active DA vector likely depends on the intensity of the toxic-forming HAB event, the length of time spent foraging in a toxic bloom, and the foraging strategy of the consumer. We chose to operationally define an active DA vector as one whose viscera content exceeds federal regulatory limits of 20 ppm (California Ocean Science Trust, 2016) and capable of transferring DA to higher trophic levels. It is also challenging to determine the effect of DA on the ecosystem because DA can enter the food web through both pelagic and benthic pathways (Vigilant and Silver, 2007). The most recognized mechanism of DA transfer to high trophic predators in pelagic regions is through primary and secondary consumers (e.g. krill, anchovies, sardines, juvenile fishes) that directly consume toxic algal cells and accumulate DA in their digestive tissues (Scholin et al., 2000; Bargu et al., 2002; Lefebvre et al., 2002b). Most of these taxa are important forage species in the California Current (Szoboszlai et al., 2015), and have been deemed the causal agent of acute and chronic DA toxicosis in California sea lions (*Zalophus californianus*), an abundant coastal marine predator often considered a sentinel for offshore DA events (Lefebvre et al., 1999; Gulland et al., 2002; Bargu et al., 2012). In contrast, Dungeness crabs are exposed to DA through benthic pathways, potentially through DA preserved and resuspended in sediments or by consuming various filter-feeding invertebrates (Lefebvre and Robertson, 2010). Our ability to predict where and when prey taxa and predators ingest DA is not fully understood, in part due to their high mobility and broad foraging areas.

DA vectors responsible for sea lion mortalities frequently focus on analyzing viscera through stomach content analysis (SCA), and urine and fecal analysis (FA). These methods provide the most consistent data, especially because DA is rapidly excreted by top predators and their prey (Gulland, 2000; Lefebvre et al., 2002b). SCA and FA offer detailed information on recently ingested prey items, and were the primary methods used to link sea lion mortality to prey with high DA concentrations (Lefebvre et al., 1999; Scholin et al., 2000). Yet, such methods poorly detect items that are highly digested and do not provide information on what or where a consumer was eating over longer time frames (Hyslop, 1980). As a result, explanations for why certain taxa are critical DA vectors to higher trophic consumers do not consider how DA varies spatially, nor do they consider how foraging strategy contributes to toxin accumulation. A more comprehensive study of taxa that accumulate DA from different habitats is necessary for understanding how DA is dispersed and transferred through marine ecosystems, and ultimately, for improving HAB response efforts.

2. Research approach & objectives

The objectives of this study are to identify key trophic pathways of DA transfer in the Monterey Bay food web and to determine the habitats and regions prone to DA accumulation during years without highly anomalous ocean conditions or major, known toxic blooms. This work incorporates a mixed method approach encompassing DA measurements and stable isotope analysis of carbon ($\delta^{13}C$) and nitrogen ($\delta^{15}N$) from animal tissues. While there have been food web studies focusing on DA in Monterey Bay (e.g. Lefebvre et al., 2002a; Bargu et al., 2002, 2008), DA measurements and isotopes have not been integrated in the same study. The combined approach presented here allows spatial variation in elemental cycling and DA accumulation in consumers to be identified and uses isotopic niches to determine important trophic links and foraging strategies that influence toxin accumulation in DA vectors from different habitats.

The $\delta^{13}C$ and $\delta^{15}N$ values offer an integrated view of the diet and habitat use of consumers (DeNiro and Epstein, 1978, 1981; Peterson and Fry, 1987). The $\delta^{13}C$ from an organism reflects the source that primary producers use for photosynthesis (Smith and Epstein, 1971) and can be used to differentiate between coastal and pelagic foragers in marine systems (Burton and Koch, 1999). Overall, higher $\delta^{13}C$ values are associated with productive regions, including coastal upwelling zones like that of the CCS (Rau et al., 1982; Goericke and Fry, 1994). The $\delta^{15}N$ values from primary producers also vary geographically based on a region's dominant N source and the degree of NO_3^- uptake by phytoplankton, relative to other sources of N (i.e., NH_4^+, NO_2^-) (Liu and Kaplan, 1989; Altabet et al., 1999). These $\delta^{13}C$ and $\delta^{15}N$ values from primary producers, referred to as baseline isotope values, vary across habitats and marine systems. Consumers integrate such information from their habitat biochemistry through their diet, allowing for source information to be inferred from animal tissues (Ruiz-Cooley et al., 2012; Ruiz-Cooley and Gerrodette, 2012). The trophic position of an organism is also reflected by the relative values of $\delta^{13}C$ and $\delta^{15}N$, given the predictable stepwise enrichment between predator and their prey (3 to 4‰ for $\delta^{15}N$, 0.5 to 1‰ for $\delta^{13}C$) (DeNiro and Epstein, 1981; Minagawa and Wada, 1984). The range of isotope values expressed in a population determines the size of its 'isotopic niche,' providing ecological information on diet and nutrient sources, trophic position, and foraging strategies (Layman et al., 2007; Newsome et al., 2007; Flaherty and Ben-David, 2010).

By relating DA measurements from potential vectors with their isotopic niche and suggested feeding behavior, we can identify species-specific foraging strategies and explain why certain consumers have a higher capacity to accumulate and transfer DA to top predators than others. We hypothesized that a species is more likely to accumulate and transport toxins throughout the food web if they are an important forage species for higher trophic level predators, have a narrow isotopic niche representing a diet specialist, and are also mobile, enabling dietary consumption over large geographic ranges. In contrast, species with broader isotopic niches whose individuals are diet generalists and

consume a wide range of prey items may be less likely to accumulate DA. Since C and N sources and cycling process vary spatially, we also expected to observe longitudinal variability in baseline isotope values and DA accumulation. Such spatial heterogeneity may reflect the inshore-offshore decoupling documented in previous studies and reveal regions where toxins accumulate in Monterey Bay (and other hotspots for DA events), even during periods without massive coastwide blooms.

3. Materials and methods

3.1. Study site and sample collection

The Monterey Bay is a highly dynamic coastal upwelling region and an ideal ecosystem to assess the accumulation of DA in consumers because the phytoplankton assemblage is dominated by diatoms, including *Pseudo-nitzschia* spp. that form toxic HABs (Garrison, 1979; Horner et al., 1997; Smith et al., 2018). Such blooms are supported by nutrient influx from seasonal, spring upwelling, and regional water circulation patterns that retain water and nutrients in parts of Monterey Bay (Rosenfeld et al., 1994; Graham and Largier, 1997; Checkley and Barth, 2009). The Monterey Bay receives additional nutrients from estuaries and rivers, including the Elkhorn Slough, San Lorenzo River, and Pajaro River, all of which are susceptible to high nutrient loads from agricultural runoff (Lane et al., 2009; Lecher et al., 2015).

Efforts to collect specimens focused on 2018, a year characterized by less anomalous oceanographic conditions following the 2014–16 large marine heatwave. HAB conditions along the coast were returning to conditions closer to the recent long-term average. Despite localized DA events in HAB hotspots, there were no region-wide HABs nor fishery closures in Monterey Bay. The Pacific Decadal Oscillation and Oceanic Niño Index were close to neutral conditions north of Point Conception in the CCS (Thompson et al., 2018; Harvey et al., 2019). Collections and sampling efforts were most comprehensive in coastal-pelagic zones and focused on potential DA vectors, including commercially important species, and California sea lions.

In this study, potential DA vectors included mussels (*Mytilus californianus*), the primary indicator of DA at coastal-benthic sites, and the northern anchovy, Pacific sardine, krill (*Euphausia pacifica* and *Thysanoessa spinifera*) and pelagic juvenile rockfish (*Sebastes semicinctus, Sebastes jordani, Sebastes saxicola,* and *Sebastes goodei*) from coastal-pelagic habitats. Market squid (*Doryteuthis opalescens*) from coastal-pelagic habitats were also included because they have high commercial value and feed at a low trophic position (Bargu et al., 2002). This collection of species are primary or secondary consumers and cover four of the five primary functional forage taxa in the CCS (Szoboszlai et al., 2015; Koehn et al., 2016). As (mostly) filter-feeders, they are are expected to be powerful DA vectors as they are the first trophic level to accumulate DA and were the primary focus of our analyses because of their comprehensive sample sizes.

All potential pelagic DA vectors were collected on the Rockfish Recruitment and Ecosystem Assessment Survey (RREAS), conducted off of California in late spring of each year (Sakuma et al., 2016). These collections occurred between 14 May and 15 June 2018, encompassed a range of depths and distance to shore gradients, and cover coastal-pelagic, coastal-benthic, and deep-benthic habitats (Fig. 1; Table 1). Extra sardine and anchovy specimens were collected between 5 May and 7 June 2019 on the RREAS, and were included to increase power of analysis. Additional krill, sardine, anchovy, and juvenile rockfish samples were obtained from the West Coast Groundfish Bottom Trawl Survey (WCGBTS) in 2018 (Appendix T1). Mussels were obtained onsite at the SCW and Moss Landing Harbor (MLH) (Fig. 1).

Additionally, species not categorized as potential vectors from benthic habitats were opportunistically collected to obtain a broader picture of the food web in Monterey Bay. These specimens include macroalgae and snails from MLH (Fig. 1) and other mollusks, benthic fish, cartilaginous fish, echinoderms, and crustaceans from WCGBTS

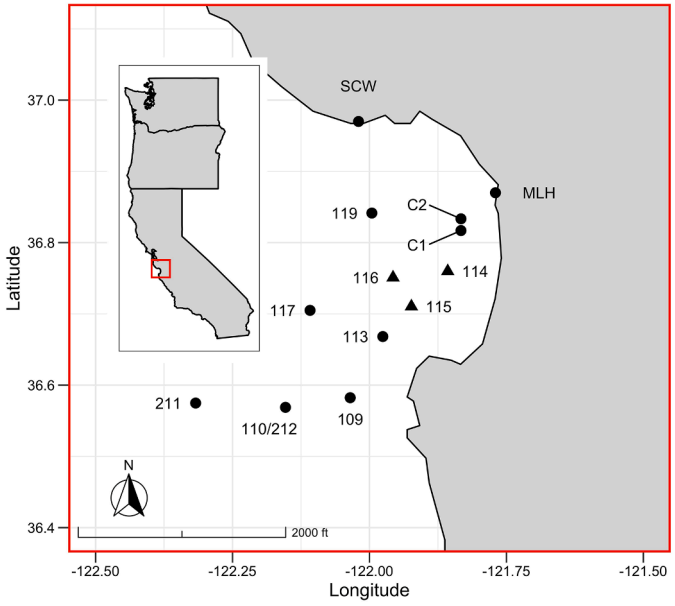

Fig. 1. Sites of specimen collections from Monterey Bay in 2018. Moss Landing Harbor (MLH). Santa Cruz Wharf (SCW). Dungeness Crab collection sites (C1,2). Stations 109–212 are the RREAS sampling sites. Triangles are stations included in the site-control analysis. Inlet map is provided to show the geographical location of Monterey Bay along the U.S. West Coast. The San Lorenzo River passes through Santa Cruz, entering the northern part of the bay. The Elkhorn Slough and Pajaro River discharge nearby MLH. Sites sampled by WCGBTS are not provided. Station depths are provided in Appendix Table 1.

Table 1
Sampling depths. Station numbers represent the original NOAA-SWFSC field station where specimens were collected (see Fig. 1). C1 and C2 are the Dungeness crab collection sites. Depths are measured in meters (m).

Station	Depth (m)
109	608
110/212	2650
113	900
114	73
115	91
116	287
117	1920
119	91
211	2516
C1	67
C2	37

(Appendix T1). Dungeness crabs were collected near Moss Landing (Fig. 1) on the R/V *Sheila B*, using recreational crab traps in June 2019 and compared with DA vectors to understand more about the feeding ecology of this commercially valuable species and a fishery that is prone to extensive closures during HABs (Ritzman et al., 2018; Holland and Leonard, 2020). While previous studies document DA presence in several of the mollusks, benthic fish, and crustaceans sampled, they were not the focus of our analyses.

Sea lion muscle and liver tissues were provided by the Marine Mammal Stranding Network at Moss Landing Marine Laboratories (MLML) and UC Santa Cruz (UCSC) under a letter of authorization from the National Oceanographic and Atmospheric Administration (NOAA). Samples were collected from freshly dead California sea lions including males and females and from a range of life history stages (yearling

through adult) who stranded in Monterey Bay between July 2017 and April 2019. Collectively, these sea lions, the potential DA vectors, and Dungeness crabs are 'key taxa' that represent a subset of the Monterey Bay ecosystem.

3.2. DA measurements and isotope analysis

DA was measured primarily from viscera to obtain information from recently ingested prey (Lefebvre et al., 1999; Gulland, 2000) using standard protocols for liquid chromatography mass spectrometry (Mekebri et al., 2009; Peacock et al., 2018). Liver tissues from stranded sea lions were measured for DA, as these were the only available tissues that offer relatively recent dietary information (days to a couple of weeks) (Vander Zanden et al., 2015). DA was measured from whole body samples of krill and soft tissue in mussels. For small individual specimens, including krill and juvenile fish that had minimal soft tissue, viscera from three to eight individuals of the same species collected at a single location were mixed for a combined DA measurement, as toxin measurements between individuals collected simultaneously are typically similar (Raphael Kudela, pers. comm.). DA measurements were not obtained from the Dungeness crabs, sardines, and anchovies collected in 2019 because of lab closures associated with the COVID-19 pandemic. Muscle tissues were separated during dissections and analyzed for C and N stable isotope analysis. A detailed description of standard laboratory processing for isotope analysis and DA measurements is available in the Appendix.

Specifically for krill, muscle and whole body were analyzed from five stations (Stations 110/212; 113; 114; 116; 117 in Fig 1) to investigate the relationship between $\delta^{13}C$ and $\delta^{15}N$ among tissues. Whole body values collected from stations (that had no muscle results) were converted into that equivalent to muscle using the least-squared regression and are the values used in all subsequent analyses (Appendix Fig. 1).

3.3. Statistical analyses

3.3.1. Community structure

The average $\delta^{13}C$ and $\delta^{15}N$ values and standard error per species were calculated for all species collected in 2018 and 2019. Isotope values from sardines and anchovies collected from 2018 to 2019 were included after interannual differences in isotope values between years were tested using one-way analysis of variance (ANOVA). A convex hull was drawn around the average values of species from each habitat (coastal-pelagic, coastal-benthic, and deep-benthic), which reflects their corresponding isotopic space (Layman et al., 2007). An ANOVA and Tukey Post Hoc Test were used to determine differences in $\delta^{13}C$ and $\delta^{15}N$ among these three habitats.

3.3.2. DA concentrations and isotope values in key taxa across habitats

To assess differences in DA accumulation among potential vectors, an ANOVA and a Tukey Post Hoc Test were used with prey species as the factor and DA concentration as the response variable. Since DA sample distributions were highly skewed, values were $\log_{10}$-transformed. To evaluate cross-shore variation in DA accumulation, a linear regression analysis evaluated DA measurements in anchovies from 2018 as a function of longitude. Anchovies were chosen for this DA regression because they can be important DA vectors in Monterey Bay (Lefebvre et al., 1999, 2002b) and were available at a sufficiently large sample size. Longitudinal variability in baseline isotope values was assessed using and values from krill muscle tissue because they are excellent proxies of baseline isotopic values and widely used to represent nutrient cycling in marine food webs (Somes et al., 2010; Espinasse et al., 2020). The average DA concentration and $\delta^{13}C$ and $\delta^{15}N$ values per composite sample at a given station were used to avoid pseudo-replication and account for dependencies between observations at a single site.

3.3.3. Trophic position estimates and the isotopic niche of key taxa

Trophic position (TP) estimates were obtained using the equation in Post (2002) for secondary consumers:

$$Trophic\ Position = \frac{[(\lambda) + (\delta^{15}N_C - \delta^{15}N_B)]}{\Delta^{15}N_C},$$

where $\delta^{15}N_C$ represents the N value of the secondary consumer. The baseline N value (i.e. mussel for coastal-benthic and krill for coastal-pelagic) and the trophic discrimination factor between a consumer and its prey (3.4‰, Post 2002) is represented by $\delta^{15}N_B$ and $\Delta^{15}N_C$, respectively. The TP of the baseline species is represented with λ. A TP of 2.2 was chosen for krill because it is the average trophic level of *E. pacifica* and *T. spinifera* from the CCS (Miller et al. 2010).

To determine the foraging strategy for each species, the isotope data were analyzed using the isotopic niche framework from Jackson et al. (2011) and Stable Isotope Bayesian Ellipses in R (SIBER) (Jackson and Parnell, 2020). The isotopic niche is represented using Bayesian multivariate standard ellipses, the bivariate equivalent to standard deviation determined through Bayesian probabilities. The ellipses were constructed around each of the eight key taxa and capture 95% of the data points for each species. A total of 100 points from the posterior values returned after 10,000 iterations were used for each ellipse. Four species of juvenile rockfish were collected and combined for analysis because they occupied similar niche spaces and have overlapping diets (Reilly et al., 1992). The two species of krill were also combined.

To statistically compare the size of each isotopic niche, Bayesian standardized ellipse areas (SEA_b) were calculated and compared using the 95% credible intervals (CI). To evaluate differences in diet and habitat, niche overlap among species was calculated by quantifying the maximum likelihood overlap between the 95% prediction ellipses. The overlap is expressed as a proportion of the non-overlapping area of two species, which provides output values ranging from 0 (distinct ellipses) to 1 (complete overlap) (Jackson and Parnell, 2020). The output values representing the proportion of non-overlapping area were multiplied by 100 and expressed as a percent. Each of the percent proportions of overlap reflect distinct feeding strategies, diet, and habitat use.

To reduce the effect of spatial variability on baseline isotope values and better evaluate foraging strategies, specifically regarding habitat use, a 'site-control analysis' was completed. This analysis consisted of the same SIBER quantifications described above; however, it was limited to a subset of individuals collected from three adjacent stations with similar bottom depths and distances to shore, and similar influences from oceanographic forces (stations 114–116; Fig. 1). A decline in SEA_b size and change in ellipse shape between the full and site-control analysis for animals with minimal mobility may indicate that the original ellipse area was influenced by heterogeneity in baseline isotope values and individual variability in diet. In contrast, no change in SEA_b size and ellipse shape would indicate that specimens comprised individual specialist feeders with less variability in their diet. Sea lions were not used in the site-control analysis because each individual was collected from a different stranding location in Monterey Bay, and whether they were residents to the region remains unknown. Mussels were excluded because of their low sample size.

Finally, the isotopic space that potential and active vectors occupy within the broader community was calculated using the SIBER framework. Bayesian standard ellipses were calculated for (i) the potential DA vectors (using each isotope value regardless of taxa; SEA_{DA}), (ii) active vectors (SEA_A), and (iii) all individual specimens collected, which represents the subsampled community in Monterey Bay (SEA_{MB}). To compare the isotopic spaces of the potential and active DA vectors with the larger community, the proportion of the SEA_{MB} represented by SEA_{DA} (and SEA_A) was calculated using the percentage overlap statistics described previously.

4. Results

4.1. Sample collection

A total of 27 fish and invertebrate species covering a range of trophic levels were collected from 13 sites (Fig. 1; Table 2; Appendix T1). The analysis consisted of 188 specimens representing 26 species collected in 2018, and 21 sardines, 21 anchovies, and 29 Dungeness crabs collected in 2019. There were no differences in $\delta^{15}N$ values between the 2018 and 2019 collections for sardines (ANOVA $F_{1,27} = 0.65$, $P = 0.8$) or anchovies ($F_{1,67} = 0.6$, $P = 0.4$ for anchovies) and the shape and size of their ellipses did not change across years, thus specimens from both years were pooled for isotope analyses.

4.2. Community structure and potential DA vectors

Fig. 2a illustrates the mean $\delta^{13}C$ and $\delta^{15}N$ values for each species. Each convex hull encompasses discrete isotope values associated with species in each habitat (Fig. 2a). A total of four species were classified as deep-benthic, eight as coastal-benthic, and ten as coastal-pelagic. Four unidentified tropical fish and one mola mola (*Mola mola)* were analyzed, but not classified in either one of the three habitats. The coastal-pelagic convex hull area was smaller than coastal-benthic and had a relatively narrow range in $\delta^{13}C$ (2.12‰) (Fig. 2a). All potential DA vectors (refer to section 2.0 for operational definition), except mussels, occupied the narrow coastal-pelagic habitat range of $\delta^{13}C$ values. The mean isotope value of these coastal-pelagic potential vectors was ~2‰ and ~4‰ lower, respectively, than for the average sea lion (Fig. 2a). There was overlap between coastal-benthic and coastal-pelagic convex hulls, but the isotope values of each species within each habitat were significantly different among them (Fig. 2a; ANOVA, $F_{3,242} = 79.01$, $P < 0.001$ for $\delta^{13}C$; ANOVA $F_{3,242} = 22.35$, $P < 0.001$ for $\delta^{15}N$). The average deep-benthic species were depleted by 1.88‰ in $\delta^{13}C$ and enriched in $\delta^{15}N$ by 2.87‰ compared to coastal-benthic species (Tukey HSD < 0.001 for $\delta^{13}C$ and $\delta^{15}N$; Fig. 2a). The average coastal-pelagic species were depleted by 0.74‰ for $\delta^{13}C$ and 3.14‰ for $\delta^{15}N$ relative to the deep-benthic (Tukey HSD < 0.001 for $\delta^{15}N$ and Tukey HSD > 0.05 for $\delta^{13}C$) and depleted by 2.62‰ and 0.27‰ for $\delta^{13}C$ and $\delta^{15}N$ relative to coastal-benthic convex hulls (Tukey HSD < 0.001 for $\delta^{13}C$ and $\delta^{15}N$).

The Bayesian metrics revealed that the potential DA vectors, which were mostly pelagic species, occupied ~40% of the community represented in this study (Fig. 2b). These DA vectors have lower trophic positions and occupy the bottom half of the $\delta^{15}N$ values from the ellipse (Fig 2b; Table 2). Anchovies collected comprised 7.96% of the isotopic community (Appendix T6).

4.3. DA concentrations and isotope values from key taxa across monterey bay habitats

DA concentrations ([DA]; ppm) were limited to samples collected in 2018. All potential DA vectors accumulated significantly different [DA] in their viscera (ANOVA, $F_{5,50} = 19.8$, $P < 0.001$). Anchovies accumulated the highest [DA] (and had the greatest variance) compared to other species (Tukey HSD, $P < 0.001$; Fig. 3) and were the only species in which individuals exceeded the active vector threshold for protecting human health. Anchovies from a single collection site had an average [DA] of 15.03 ppm, which is 10x greater than that accumulated in any other potential vectors (Fig. 3; Appendix T1). Sardines recorded the second highest average [DA] of all potential vectors, and krill accumulated the least (Fig. 3). Juvenile rockfish, market squid, and mussels recorded similarly low levels of DA, ranging from 0.21 to 0.29 ppm (Fig. 3: Appendix T1). Sea lion livers contained the least [DA] of all taxa and tissue type (Fig. 3). Certain coastal-benthic and deep-benthic species, including prawns, sanddabs, and grenadier, had comparable [DA] in their viscera to some potential pelagic DA vectors (Fig. 3; Appendix

Table 2
Estimated trophic position of the potential vectors and California sea lions. Trophic position (TP) was estimated following Post (2002)'s equation in section 2.2.3. The mean C:N ratio and standard deviation (SD) is shown for all specimens of the given species analyzed.

Species	TP	Mean C:N (SD)
Anchovy	3.08	3.74 (1.45)
Krill	2.2	3.66 (0.19)
Juvenile rockfish	2.87	3.63 (0.17)
Sardine	2.95	3.44 (0.25)
Market squid	2.93	3.47 (0.05)
Mussel	2.2	3.87 (0.17)
Sea lion	4.16	3.29 (0.19)
Dungeness crab	3.46	3.22 (0.07)

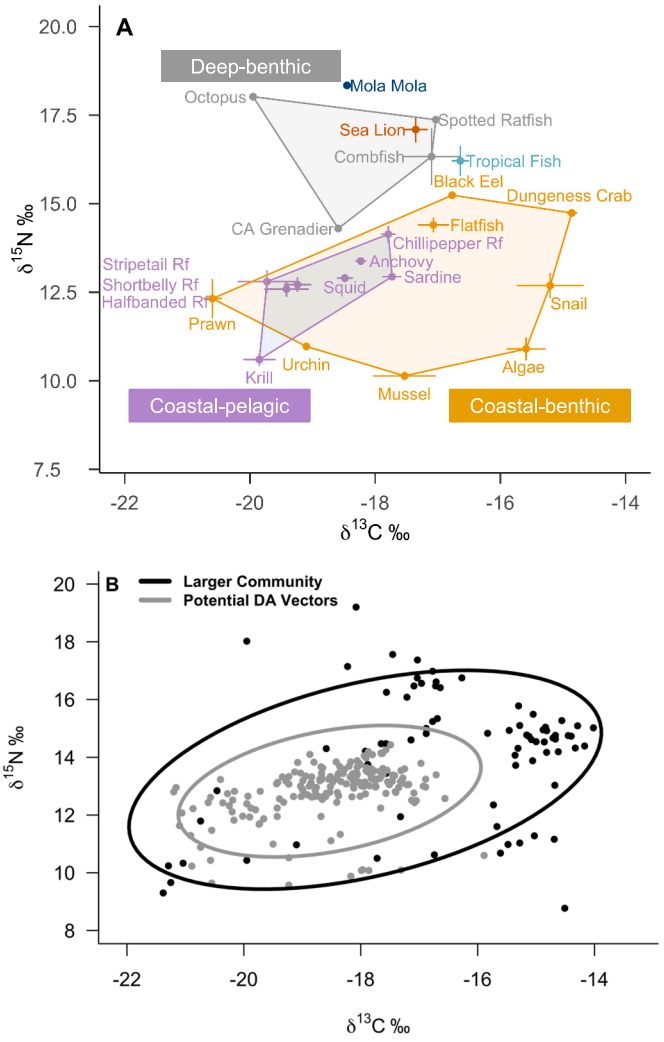

Fig. 2. Community structure. (A) The average $\delta^{13}C$ (‰) and $\delta^{15}N$ (‰) values of all species collected in Monterey Bay from 2017 to 2019. Each point represents the mean value for each species (± standard error). Convex hulls surround the mean values of species in their corresponding foraging habitat: coastal-benthic in orange, coastal-pelagic in purple, deep-benthic in gray. Stranded sea lions in red were excluded from convex hulls because they can feed on prey from any of these habitats. Tropical fish in turquoise were also excluded from convex hulls because they were not identified at the species level and could be transitory, as with *Mola mola* in dark blue. Rf refers to rockfish. (B) Comparison of Bayesian standard ellipses between the whole community (all specimens analyzed in this study; black) and the potential DA vectors (gray). Each point represents the isotope value per individual. (To interprate the references to colour in this figure legend, refer the web version of this article.)

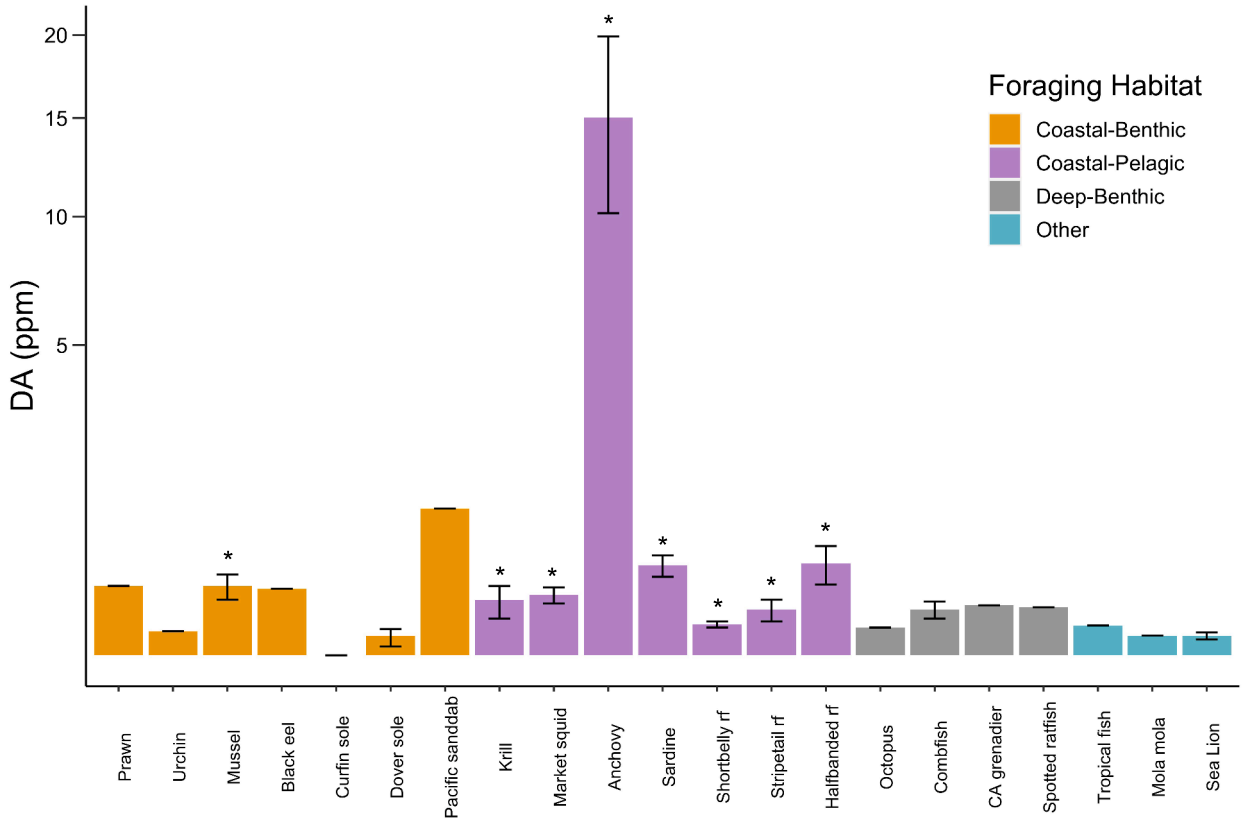

Fig. 3. DA measurements among taxa. The average DA concentrations (ppm) of all species analyzed for DA (± standard error) in this study. Colors indicate foraging habitat (see methods and Fig. 2a). Species considered to be potential DA vectors, according to our working definition, are indicated with an * . Other species were included for comparison and to illustrate the presence of DA during years without documented surface blooms. (To interprate the references to colour in this figure legend, refer to the web version of this article.)

T1), although they were not the primary focus of this study.

A negative relationship between DA accumulation in anchovies and longitude (representing a coastal to offshore gradient) was documented: anchovies collected at central and southern sampling sites inside Monterey Bay had higher [DA] than those further offshore (Linear Regression, $F_{1,6} = 5.75$, $P = 0.05$, $r^2 = 0.48$; Fig. 4a). A negative linear relationship between $\delta^{13}C$ in krill and longitude was also observed (Linear Regression, $F_{1,5} = 8.45$, $P = 0.03$, $r^2 = 0.63$; Fig. 4b), but $\delta^{15}N$ in krill did not vary with longitude (Linear Regression, $F_{1,5} = 0.03$, $P = 0.85$, $r^2 = 0.01$). These krill regressions incorporated $\delta^{13}C$ and $\delta^{15}N$ from whole bodies of krill, which were converted into muscle values using the equations $\delta^{13}C_{muscle} = [(\delta^{13}C_{whole} - 5.18)/1.13]$ and $\delta^{15}N_{muscle} = [(\delta^{15}N_{whole} - 1.8265)/0.8983]$, as there was a positive linear relationship between $\delta^{13}C$ and values from whole body and muscle (Appendix Fig. 1; Linear Regression, $F_{1,5} = 63.58$, $P = 0.001$, $r^2 = 0.92$ for $\delta^{13}C$; $F_{1,5} = 36.73$, $P = 0.003$, $r^2 = 0.87$ for $\delta^{15}N$). This allowed for whole-body tissue from krill to be used from stations where muscle was not collected.

4.4. Isotopic niche, trophic position, and DA accumulation of key taxa

Among DA vectors, anchovies and market squid had the highest degree of ellipse overlap (50%), followed by market squid and sardines (46.23%), anchovies and sardines (40%), and market squid and juvenile rockfish (38.5%) (Fig. 5a, Appendix T4). These four species occupied similar isotopic niches and had similar average $\delta^{15}N$ values and trophic positions (Fig 5a,c; Table 2). The smallest degree of overlap was between juvenile rockfish and market squid, and market squid and krill (13.8% and 4.19%; Appendix T4). Krill did not overlap with sardines nor anchovies (Fig. 5a). Even though anchovies and market squid overlapped by 50% (Fig. 5a), market squid accumulated the least DA (0.19 ppm) of all coastal-pelagic foragers, while anchovies accumulated the most (Fig 3; Fig. 5a; Appendix T1).

Sardines and anchovies had similar trophic positions and exhibited ellipses that were moderately wide, with narrow ranges of $\delta^{15}N$ that resulted in a compressed isotopic niche (Fig. 5a; Table 2). The shape of their ellipse remained similar when their data points were reduced in the site-control analysis (Fig. 5b). Anchovies had a slightly higher raw mean and smaller variance in SEA_b than sardines and accumulated significantly more DA (Fig. 3; Appendix T5; Appendix Fig. 2). Results from the raw mean SEA_b (without considering the 95% CI) showed that anchovies and sardines have smaller SEA_b than market squid or moderately mobile species like krill and juvenile rockfish (Appendix T3,4).

Mussel and krill ellipses exhibit relatively large ranges of $\delta^{13}C$ values (~6‰ and >5‰) from broad contributions of carbon sources (Fig. 5a). Mussels contained the third highest DA concentration (Fig. 3), the lowest $\delta^{15}N$ values and trophic position among potential vectors, and the narrowest range in $\delta^{15}N$ (< 1‰), leading to the most compressed ellipse among taxa (Fig. 5a). Based on the 95% credible intervals, average SEA_b values of mussels are similar to that of sardines and anchovies, but smaller than mussels (Appendix T4). The wide range in $\delta^{13}C$ and $\delta^{15}N$ values for muscle in krill is consistent with krill occupying a large isotopic niche, although they have the least DA of all potential vectors and the lowest trophic position among the pelagic vectors (Fig. 3; Fig. 5a). While the range in $\delta^{13}C$ appears to be reduced between the full and site-control analysis, the mean SEA_b, and shape and orientation of the krill ellipse did not change (Fig. 5; Appendix T4,6).

The trophic position estimate for juvenile rockfish was comparable to market squid, but market squid had a narrower $\delta^{15}N$ range (Table 2; Fig. 5a). The juvenile rockfish ellipse exhibited the largest range in $\delta^{15}N$ (~4.5‰) of the potential DA vectors and the widest range in $\delta^{13}C$ values

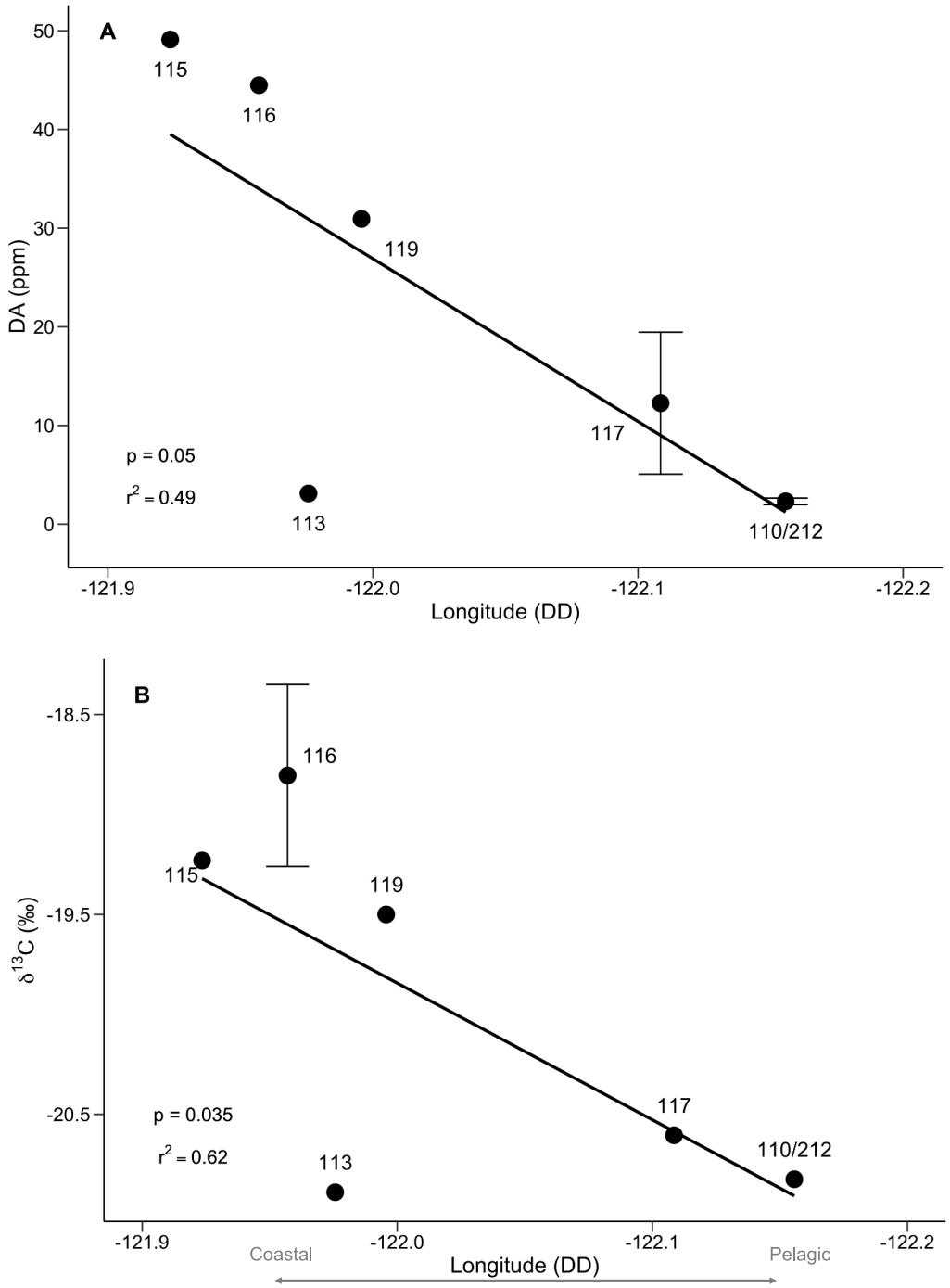

Fig. 4. Spatial variation in DA and baseline isotope values. Regression analyses showing the association between (A) the average DA concentrations (ppm) of anchovies and longitude of collection site and (B) the average $\delta^{13}C$ (‰) from krill muscle tissue and longitude. Station numbers correspond to those depicted in Fig. 1. Error bars represent standard error at stations with multiple samples.

(~6‰) of all taxa analyzed, resulting in the highest mean SEA_b and largest isotopic niche (Table 2; Fig. 5a). Their mean SEA_b declined from 2.18 with the full dataset to 0.81 in the site-control analysis (Fig. Fig. 5; Appendix T4,6). Market squid had a relatively small mean SEA_b that also declined from 0.7 in the full analysis to 0.13 in the site-control analysis (Appendix T4,6).

Dungeness crabs had a round ellipse with similar $\delta^{13}C$ and $\delta^{15}N$ ranges (Fig. 5a). The SEA_b for crabs is comparable to that for sardines and anchovies despite their higher trophic position (Table 2; Appendix T4, Fig. 2). Stranded sea lions accumulated minimal DA and occupied the highest trophic level (Fig. 3; Table 2). They are enriched by ~3–4‰ in $\delta^{15}N$ compared to the mid-trophic foragers and possess an ellipse with the greatest range in $\delta^{15}N$ (~6‰) (Fig 5a). Unlike the potential DA vectors and Dungeness crabs, sea lions have a wider range in $\delta^{15}N$ than $\delta^{13}C$, resulting in a more vertically shaped ellipse (Fig. 5a).

5. Discussion

This is the first study to combine isotope analysis with DA measurements to evaluate variability in DA accumulation across habitats, species, and trophic levels. Below, we discuss isotope results from all specimens collected in 2018 and 2019, the variation in DA

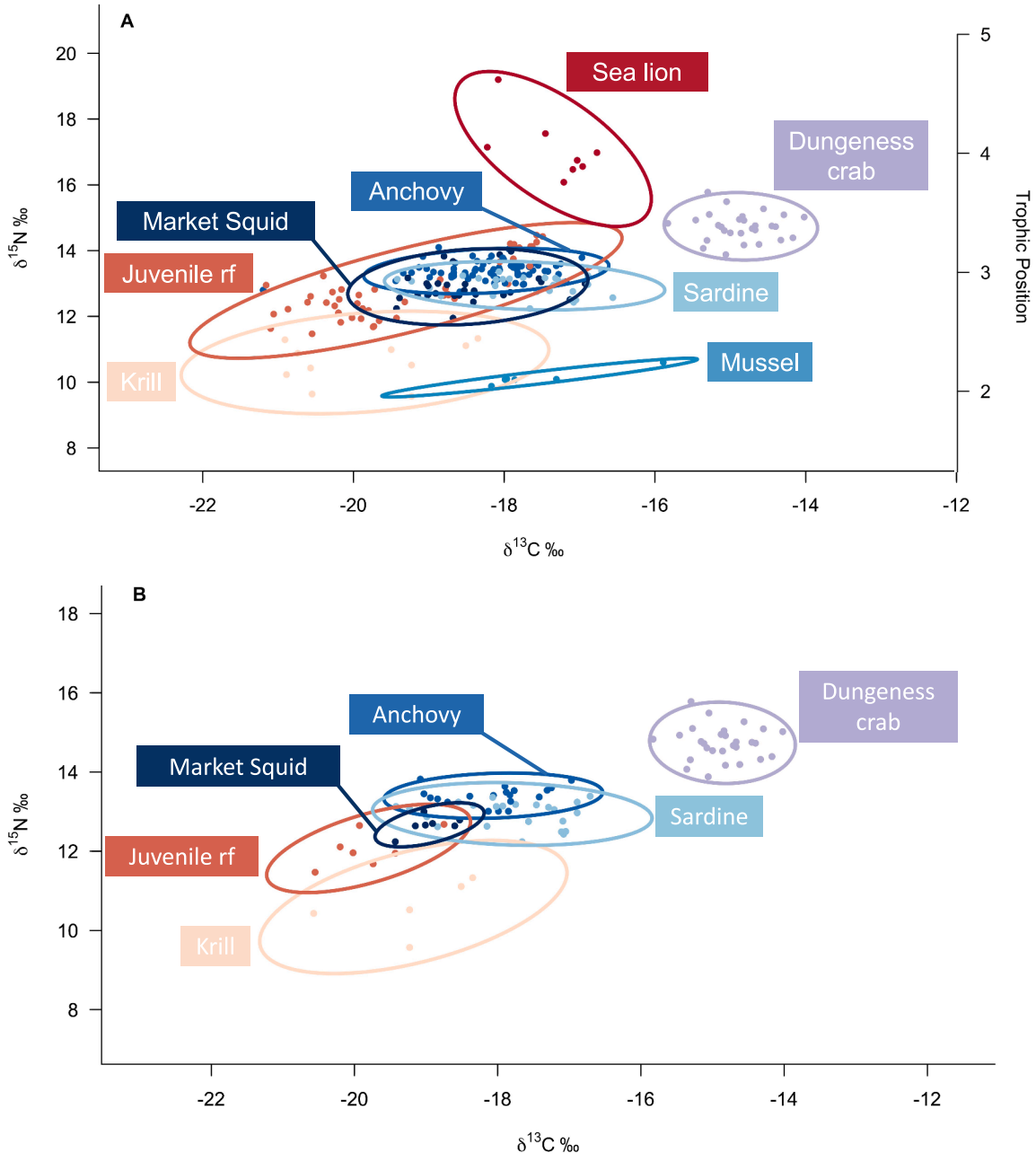

Fig. 5. Isotopic niches of potential DA vectors, crabs and predators vulnerable to DA toxicosis. (A) Bayesian standard ellipses and trophic level estimates of key taxa. Each point represents an individual and each color is associated with a different species. (B) Site-control analysis presenting the Bayesian ellipses of five potential DA vectors collected at stations 114, 115, and 116, and Dungeness crabs at C1 and C2 (see Fig. 1).To interpret the references to colour in this figure legend, refer to the web version of this article.

accumulation, and interpret the feeding strategies of key taxa. Our study provides insight into the community structure and different baseline isotope values among habitats (Fig. 2), highlights inshore-offshore gradients in isotope values and DA accumulation in Monterey Bay (Fig. 4), and reveals differences in toxin accumulation (Fig. 3) and foraging strategies across taxa. These results have implications for reconstructing the food web and for identifying routes of DA trophic transfer.

5.1. Variation in baseline isotope values reveals differences in community structure and biochemical processes among habitats

The isotopic differences among the three convex hulls suggests that distinct elemental cycling processes dominate in each habitat, driving unique baseline C and N isotope values. The wide range in $\delta^{13}C$ for the coastal-benthic convex hull (5.7‰) could be driven by a mix of carbon sources and primary productivity (Peterson and Fry, 1987). The coastal-pelagic zone had the narrowest convex hull (2.12‰), but krill

from these habitats reflect a significant inshore-offshore gradient in $\delta^{13}C$. Longitude explains 63% of this spatial variation (Fig. 4b). Krill collected from lower longitudes, at central and southern stations inside Monterey Bay had higher $\delta^{13}C$ values than those in pelagic zones. Since krill are primary consumers and are not thought to actively move horizontally, they likely reflect source information integrated from the water mass in which they reside, thus suggesting differences in C fixation and cycling.

The observed longitudinal gradient in $\delta^{13}C$ in coastal-pelagic habitats may be driven by variation in community composition of primary producers and primary productivity. Phytoplankton type, size, growth rate, and photosynthetic pathway can determine the degree of isotopic fractionation (Smith and Epstein, 1971; Peterson and Fry, 1987). Larger cell phytoplankton, such as *Pseudo-nitzschia* diatoms, have faster growth rates and are enriched in ^{13}C, and thus have higher $\delta^{13}C$ compared to slower growing, smaller phytoplankton (Goericke and Fry, 1994). The water inside Monterey Bay provides the necessary nutrients to support larger biomass phytoplankton (Wilkerson et al., 2001). This results from seasonal upwelling, when bands of nutrient rich water move across the bay and bifurcates (Rosenfeld et al., 1994). Some of this water remains trapped inside Monterey Bay, allowing larger celled phytoplankton to thrive, thus yielding higher $\delta^{13}C$ values in krill. In contrast, water masses outside the mouth of Monterey Bay are less productive and favor lower biomass primary producers with lower $\delta^{13}C$ values (Rosenfeld et al., 1994; Wilkerson et al., 2000)

The oceanographic processes and productivity gradients that influence spatial variability in $\delta^{13}C$ may also contribute to the decoupling of inshore and offshore blooms. In fact, the four groups of anchovies that accumulated >20 ppm were collected inside Monterey Bay, at sites where krill were enriched in $^{13}C^{13}C$ (albeit $\delta^{13}C$ from krill may capture a different integration time than accumulation of DA in viscera) (Fig. 1,4; Appendix T2). The nutrient-rich water from seasonal upwelling that remains trapped inside Monterey Bay continually recirculates (Paduan and Rosenfeld, 1996), possibly fueling toxigenic *Pseudo-nitzschia* blooms. On the other hand, water masses outside of Monterey Bay receive greater influence from the larger moving CCS, which moves faster and in a less cyclical manner creating conditions less favorable for nutrients to support *Pseudo-nitzschia* blooms (Rosenfeld et al., 1994; Paduan and Rosenfeld, 1996). Since DA-producing *Pseudo-nitzschia* blooms are sensitive to small-scale oceanographic features (Ryan et al., 2005, 2014; Lewitus et al., 2012; Trainer et al., 2012), it may be possible for enriched ^{13}C values in regions inside of Monterey Bay (or the oceanographic conditions that produce such differences) to be characteristic of toxic *Pseudo-nitzschia* blooms.

For N, different $\delta^{15}N$ values among species and among convex hulls imply that these habitats are dominated by distinct N sources and cycling processes, because $\delta^{15}N$ from marine species reflects information on their diet and foraging habitats (Ruiz-Cooley et al., 2012). Octopus and ratfish had higher $\delta^{15}N$ values than their potential predator, the sea lion (Fig. 2a). The long-held assumption that $\delta^{15}N$ increases with trophic level (Minagawa and Wada, 1984) would stipulate that octopus are feeding at higher trophic levels than sea lions, however, our findings suggest variation in baseline $\delta^{15}N$ values between deep-benthic and the coastal habitats explains the departure from canon. Deeper waters are usually enriched in N by up to 5–10‰ because ^{14}N is lost faster than ^{15}N during particulate N decomposition at depth, as identified in the northeast Indian Ocean (Saino and Hattori, 1980; Peterson and Fry, 1987). Such ^{15}N enrichment in deeper habitats may be associated with remote upwelling sources from the northward moving California undercurrent that influences depths >30 m in Monterey Bay (Liu and Kaplan, 1989; Altabet et al., 1999). If deep-benthic regions are enriched in ^{15}N, the consumers foraging in such habitats should be as well. Therefore, $\delta^{15}N$ values from consumers feeding in coastal-pelagic, deep-benthic, or coastal-benthic regions (from tissues that reflect information from the most recently ingested meal) could potentially help identify the foraging grounds of mobile animals containing DA, including stranded marine mammals with DA toxicosis.

5.2. Variation in DA accumulation across habitats and taxa

Small pelagic fish that were potential vectors accumulated higher concentrations of DA than most taxa from other habitats (Fig. 3). The benthic species with similar [DA] to pelagic vectors and mussels, such as sanddabs, prawns and grenadier, may have acquired DA from toxic sinking particulate matter, including *Pseudo-nitzschia* spp. cells or fecal pellets from planktivorous feeders, or through resuspending and ingesting toxins that accumulated in the sediment from previous DA events (Lefebvre et al., 2002a; Vigilant and Silver, 2007). It is also known that toxic cells rapidly flocculate to the seafloor (Sekula-Wood et al., 2009; Umhau et al., 2018). Since anchovies accumulated high DA concentrations in their viscera, it is possible that newly produced toxic blooms were likely present in the water column where they fed, despite the lack of DA detected by routine CDPH shore monitoring and no documented region-wide blooms within the region of study and time frame (Thompson et al., 2018; Harvey et al., 2019; R. Kudela, pers. comm). Anchovies potentially accumulated toxins from directly ingesting toxic cells in cryptic subsurface layers (McManus et al., 2008), given that DA was not present in krill, an intermediary source of DA. Anchovies were also the only species with DA concentrations exceeding the federal regulatory limits (20 ppm), indicating that, at times, they may be the most powerful DA vector in coastal-pelagic, upwelling regions such as Monterey Bay. Their role as a DA vector could result from their foraging strategies described in Section 4.2.

The differences in DA accumulation between anchovies and mussels are consistent with previously observed decoupling between offshore and nearshore coastal environments in the southern CCS (Kudela et al., 2012; Frolov et al., 2013; Umhau et al., 2018). The spatial mismatches and patchy distribution of HAB species and DA production renders 'fixed point' nearshore monitoring, like that used for mussels, insufficient for identifying presence or absence of DA in the CCS given the dynamic coastal processes that characterize hotspots, including the Monterey Bay (Ryan et al., 2011). Our findings confirm these claims: anchovies collected on May 15 and 16, 2018 contained 28 to 49 ppm of DA, while mussels from the SCW on the same date only contained 0.42 ppm (R. Kudela, unpublished data). Anchovies, like mussels, capture instantaneous shifts in the environment because DA in their viscera represents recently ingested toxins and is depurated quickly (Lefebvre et al., 2002b). Collectively, our results indicate that anchovies are good indicators of DA in non-coastal waters where routine shoreline monitoring initiatives would fail to detect these events, further highlighting the limitations of relying on mussels as the only or primary indicator species for DA presence in a given ecosystem.

Minimal DA was detected in liver samples from sea lions (Fig 3). Liver is not the optimal tissue to detect DA (Gulland, 2000), but was selected for analysis because it reflects recent dietary sources (over a scale of days) and was readily available (Vander Zanden et al., 2015). The trace levels of DA in their liver are consistent with their necropsy reports indicating no signs of DA toxicosis (R. Dunkin, pers. comm.). It also aligns with findings from sea lions over a geographic range extending beyond Monterey Bay (Greig et al., 2005; Goldstein et al., 2008). The number of admitted sea lions in central California with confirmed or suspected DA toxicosis symptoms in 2018 was close to the median number of animals, relative to a 1998–2019 baseline (C. Field, TMMC, pers. comm.), suggesting that the populations of sea lions in these regions were not exposed to particularly high DA levels during the study period.

5.3. Isotopic niche and DA concentrations reveal the foraging strategies of key vectors

The foraging strategy (i.e. dietary and habitat generalist or specialist) of key taxa was determined using the size (SEA_b), shape, and orientation

of each species' isotopic niche and ellipse. In the wild, a smaller SEA_b may indicate a group of specialist feeders that integrates source information from similar prey. A broad isotopic niche with a relatively large SEA_b and wider range in $\delta^{15}N$ values than $\delta^{13}C$ may reflect a population of generalist consumers, with individuals who have different diets and forage in isotopically distinct regions (Layman et al., 2007; Newsome et al., 2009). Habitat generalists that are diet specialists may display a narrower niche width and smaller SEA_b than habitat specialists because generalists integrate prey and nutrients from a variety of baseline source values (Flaherty and Ben-David, 2010). These classifications were used in conjunction with known information on the diet and feeding capacity to interpret the foraging strategy for key taxa (Appendix T2).

Mussels had the most compressed ellipse of all potential vectors, indicating diet specialization, a strategy for sessile mollusks whereby they only consume microorganisms of a particular size class and detritus suspended in the water column at their site of attachment (Fox and Coe, 1943). The wide range in $\delta^{13}C$ results from mussels being collected at two locations with different primary producers and C inputs. Similar to $\delta^{13}C$ being a site-specific signal, DA concentrations from mussels are also site-specific because mussels are sessile and accumulate and depurate DA faster than other bivalves (Wohlgeschaffen et al., 1992). While they are good sentinels for public health at a local scale, our results indicate that mussels did not capture toxins during low DA years nor the C or N sources that are further offshore (Fig. 3).

Unlike mussels, Dungeness crabs are not considered potential vectors using our working definition but are known to accumulate DA and act as vectors to humans and other predators, and have a round ellipse. Their high $\delta^{15}N$ values result from consuming a broad array of teleost fish and invertebrates from the benthos (including potential vectors, like mussels) and scavenger-like behavior (Stevens et al., 1982). Krill, market squid, and juvenile rockfish had relatively large ellipse areas and wider ranges in N compared to other coastal pelagic-vectors, suggesting that the individuals consumed different prey items or fed at sites with distinct baseline values, thus resembling generalist consumptive patterns. The isotopic niche of krill and consistency in niche shape and SEA_b between the site-control and full analysis reflects the fact that krill are restricted to feeding within a defined water mass. While krill feed opportunistically, their limited mobility (Brinton, 1962; Gómez-Gutiérrez et al., 2005; Cimino et al., 2020) prevents them from capturing toxins from as broad a region in coastal-pelagic zones as highly mobile foragers such as anchovies or from being proxies for a single habitat as seen for mussels.

Market squid and juvenile rockfish ellipses declined between the full and site-control analysis, primarily by a reduced range in $\delta^{13}C$ and a small decline in $\delta^{15}N$, indicating that their original SEA_b was partially driven by specimens being collected from multiple geographic regions with varying baseline values. The reduced ellipse for market squid in the site-control analysis suggests that individuals from the same collection site fed on prey from a single trophic level and a given region, as they can be restricted to feed in a single water mass and on dense patches of krill, copepods, and megalop larvae (Karpov and Cailliet, 1979; Ish et al., 2004). Juvenile rockfish may be less mobile than squid, but are also opportunistic in that they consume pelagic copepods, krill, and krill eggs, depending on what is seasonally abundant (Reilly et al., 1992). The juvenile rockfish may represent a planktivorous foraging guild of generalist individuals who consume available prey, as they had a wide, ~3‰ range in $\delta^{15}N$. Interestingly, market squid and juvenile rockfish had minimal toxins, even on from hauls where anchovies detected high [DA], suggesting that despite their ability to accumulate DA in Monterey Bay (Bargu et al., 2002, 2008), they were not at this time.

The isotopic niche data from anchovies and sardines suggest they are both dietary and habitat specialists, likely feeding across a wide geographic range along the coastline. They migrate extensively between spawning locations and pelagic feeding sites, and integrate nutrient sources from diverse regions (but within the same coastal-pelagic habitat) through their diet, which may contribute to their wide range in $\delta^{13}C$ (Rykaczewski and Checkly, 2008; Van Der Lingen et al., 2009). The overlap in isotopic space between sardines and anchovies and similar trophic positions support that they have similar foraging strategies; however, their differences in DA levels indicate an important degree of resource partitioning at the baseline level.

The resource partitioning between sardines and anchovies may result from morphological restrictions and feeding patterns, and there is a precedent for similar filter feeding taxa to respond differently to HABs as a result such differences in morphology and foraging. Anchovies are size-selective feeders with coarse gill rakers who preferentially ingest larger prey, including larger copepods and phytoplankton. They generally thrive in nutrient rich, highly turbid, upwelled water that supports large-celled diatoms, including toxin-producing *Pseudo-nitzschia* spp. (Rykaczewski and Checkley, 2008; Zwolinski et al., 2012). Based on stomach content analysis, diatoms are the dominant phytoplankton in their diets (Van Der Lingen et al., 2006; Espinoza et al., 2009). The toxic *Pseudo-nitzschia* spp. may be ingested by anchovies directly via filter feeding or indirectly through copepods containing DA. The size range of *Pseudo-nitzschia* spp. falls within the scope when anchovies and sardines filter feed, but toxic *Pseudo-nitzschia* cells may be less available to sardines during filter feeding. Sardines have finer gill rakers that make it easier to retain smaller particles (Van Der Lingen et al., 2016) and their morphological restrictions make it more energetically efficient to occupy, as well as migrate to, more offshore regions with warmer environments (Rykaczewski and Checkley, 2008; Zwolinski et al., 2012) where toxin-producing *Pseudo-nitzschia* blooms are less frequent. Similarly, the phytoplankton in the diet of sardines is dominated by dinoflagellates, and less so by diatoms (Van Der Lingen, 2002; Van Der Lingen et al., 2006). These characteristics may contribute to sardines retaining less DA and depurating toxins faster than anchovies. While these explanations are uncertain and warrant future research, they are highly consistent with existing literature and the general notion that the diet and distribution of sardines and anchovies are distinct.

The finding that anchovies were more efficient DA vectors than sardines because of resource partitioning is consistent with Lefebvre et al. (2002b). These authors found that *Pseudo-nitzschia* spp. cell densities and DA levels were twice as high in anchovies compared to sardines collected simultaneously and suggested that anchovies were feeding exclusively on diatoms, while sardines were feeding on zooplankton with less DA. More recent research indicates that sardines and anchovies are opportunistic foragers, partition prey based on size class, and occupy different trophic positions (Van Der Lingen et al., 2006; Miller and Brodeur, 2007; Checkley et al. 2009). Our results partially disagree with these findings: the selection of prey based on size can potentially explain their distinct capacities to accumulate DA, but both species have the same trophic level in our study.

The isotopic niche data for sea lions and ability to forage across large spatial scales suggests that they have generalist tendencies. The stranded sea lions could be from a broader population of mobile individuals that integrate source information from a range of habitats and prey throughout the CCS, driving their wide range in $\delta^{13}C$ and $\delta^{15}N$ between individuals. They could be also individual specialists who opportunistically exploit what is seasonally abundant and forage throughout the continental shelf, integrating a variety of baseline N values (Lowry et al., 1991; Weise and Harvey, 2008). This specialization at an individual level could explain the vertically shaped ellipse, cluster of individuals with similar isotope values against outliers, and high variance in SEA_b. The variance could also result from a heterogenous sampling scheme that encompasses male and female individuals who forage between 90 and 650 km from shore (Costa et al., 2007) and may not be residents of Monterey Bay. Given the high mobility of sea lions and that an individual may opportunistically feed over broad spatial scales, it may be difficult to use sea lions as a sentinel species for DA warnings at the local scale, but they are extremely useful for capturing broad ecosystem-level variability in phycotoxin production.

6. Summary and management implications

The ability to predict and respond quickly to HAB events and manage human health and wildlife threats requires knowledge of the main DA vectors and their foraging patterns, especially in regional hotspots for DA outbreaks. This study illustrates the efficacy of using DA measurements from tissues with fast turnover rates, and $\delta^{13}C$ and $\delta^{15}N$ from bulk tissue samples of a wide range of taxa, to identify the main vectors of DA transfer during a period without coast-wide toxic blooms nor highly anomalous oceanographic conditions. Ultimately, this approach allowed us to identify the habitats where DA was potentially produced and accumulated in consumers: coastal-pelagic regions. It also enabled us to determine the primary route of toxin transfer during summer 2018: via newly produced blooms in the euphotic zone and the direct accumulation of DA by anchovies.

Isotope results from krill suggest an important link between coastal productivity and DA accumulation. The $\delta^{13}C$ in primary consumers like krill should be used systematically to evaluate spatial differences in elemental cycling that might be linked to sites of *Pseudo-nitzschia* blooms and DA events in non-coastal zones. Additionally, the variation in baseline $\delta^{15}N$ values among habitats in Monterey Bay can be used to identify the habitat of resident consumers that have accumulated high levels of DA, thus providing evidence of regions affected by DA. By knowing when a given habitat has been impacted by DA at a given point in time, fishery closures can be more targeted, which will reduce economic hardships to local communities.

Our study highlights subtle but important differences in anchovy foraging strategies that make them more suitable indicators of DA presence in coastal-pelagic regions than other forage species like market squid, juvenile rockfish, and krill, and true specialists like mussels. Anchovies occupy critical intermediate trophic positions, are important prey for a variety of predators, and transfer energy and biomass to higher trophic levels in upwelling systems such as the CCS (Ryther, 1969; Rykaczewski and Checkley, 2008; Szoboszlai et al., 2015). As they are fairly mobile schooling fish and potential prey of many piscivorous predators, anchovies may rapidly disperse DA throughout the food web (Madigan et al., 2012; Szoboszlai et al., 2015; Koehn et al., 2016). ws Since anchovies have potential to serve as DA vectors, we strongly recommend incorporating DA measurements from anchovies into routine sampling procols as complementary indicator species to mussels to monitor for DA presence and accumulation in coastal-pelagic regions.

Declaration of Competing Interest

The authors declare that they have no known competing financial interests or personal relationships that could have appeared to influence the work reported in this paper.

Acknowledgements

This research was supported by the California Sea Grant R/HCE-05. We thank the Captain, Crew and Scientists from the Rockfish Recruitment and Ecosystem Assessment surveys in 2018 and 2019, and D. Kamikawa (NOAA; NMFS) and J. Cordova (Moss Landing Marine Laboratories; MLML) for their support during the 2018 collections on West Coast Groundfish Bottom Trawl Surveys. We also extend our thanks to K. Negrey (UCSC) for helping analyze DA concentrations, S. Hsu and M. Jew (MLML) for sample preparation, and MLML marine operations on the R/V *Sheila B* for field work Dungeness crab collections under sport permit 1066991024. We thank K. Wirga and A. Diluzio (UCSC Marine Mammal Stranding Network) for providing sea lion tissue samples.

Supplementary materials

Supplementary material associated with this article can be found, in the online version, at doi:10.1016/j.hal.2021.102117.

References

Altabet, M.A., Pilskaln, C., Thunell, R., Pride, C., Sigman, D., Chavez, F., Francois, R., 1999. The nitrogen isotope biogeochemistry of sinking particles from the margin of the eastern North Pacific. Deep. Res. Part I Oceanogr. Res. Pap. 46, 655–679.

Anderson, C.R., Berdalet, E., Kudela, R.M., Cusack, C.K., Silke, J., O'Rourke, E., Dugan, D., McCammon, M., Newton, J.A., Moore, S.K., Paige, K., Ruberg, S., Morrison, J.R., Kirkpatrick, B., Hubbard, K., Morell, J., 2019. Scaling up from regional case studies to a global harmful algal bloom observing system. Front. Mar. Sci. 6.

Anderson, C.R., Kudela, R.M., Kahru, M., Chao, Y., Rosenfeld, L.K., Bahr, F.L., Anderson, D.M., Norris, T.A., 2016. Initial skill assessment of the California harmful algae risk mapping (C-HARM) system. Harmful Algae 59, 1–18.

Bargu, S., Goldstein, T., Roberts, K., Li, C., Gulland, F.M.D., 2012. *Pseudo-nitzschia* blooms, domoic acid, and related California sea lion strandings in Monterey Bay. California. Mar. Mammal Sci. 28, 237–253.

Bargu, S., Powell, C.L., Coale, S.L., Busman, M., Doucette, G.J., Silver, M.W., 2002. Krill: a potential vector for domoic acid in marine food webs. Mar. Ecol. Prog. Ser. 237, 209–216.

Bargu, S., Powell, C.L., Wang, Z., Doucette, G.J., Silver, M.W., 2008. Note on the occurrence of *Pseudo-nitzschia australis* and domoic acid in squid from Monterey Bay, CA (USA). Harmful Algae 7, 45–51.

Bates, S.S., Bird, C.J., de Freitas, A.S.W., Foxall, R., Giligan, M., Hanic, L.A., Johnson, G. R., McCulloch, A.W., Odense, P., Pocklington, R., Quilliam, M.A., Sim, P.G., Smith, J. C., Subba Rao, D.V., Todd, E.C., Walter, J.A., Wright, J.L., 1989. Pennate diatom *Nitzschia pungens* as the primary source of domoic acid, a toxin in shellfish from eastern Prince Edward Island. Canada. Can. J. Fish. Aquat. Sci. 46.

Bowers, H.A., Ryan, J.P., Hayashi, K., Woods, A.L., Marin, R., Smith, G.J., Hubbard, K.A., Doucette, G.J., Mikulski, C.M., Gellene, A.G., Zhang, Y., Kudela, R.M., Caron, D.A., Birch, J.M., Scholin, C.A., 2018. Diversity and toxicity of *Pseudo-nitzschia* species in Monterey Bay: perspectives from targeted and adaptive sampling. Harmful Algae 78, 129–141.

Brinton, E., 1962. The distribution of Pacific Euphausiids.

Burton, R.K., Koch, P.L., 1999. Isotopic tracking of foraging and long-distance migration in northeastern Pacific pinnipeds. Oecologia 119, 578–585.

California Ocean Science Trust, 2016. Frequently asked questions: harmful algal blooms and California fisheries.

Checkley, D.M., Barth, J.A., 2009. Patterns and processes in the California current system. Prog. Oceanogr. 83, 49–64.

Cimino, M.A., Santora, J.A., Schroeder, I., Sydeman, W., Jacox, M.G., Hazen, E.L., Bograd, S.J., 2020. Essential krill species habitat resolved by seasonal upwelling and ocean circulation models within the large marine ecosystem of the California Current System. Ecography (Cop.) 43, 1536–1549.

Costa, D.P., Kuhn, C.E., Weise, M.J., 2007. Foraging ecology of the California sea lion: diet, diving behavior, foraging location, and predation impacts on fisheries resourceshttps://escholarship.org/uc/item/9gr5784d.

DeNiro, M.J., Epstein, S., 1981. Influence of diet on the distribution of nitrogen isotopes in animals. Geochim. Cosmochim. Acta 45, 341–351.

DeNiro, M.J., Epstein, S., 1978. Influence of diet on the distribution of carbon isotopes in animals. Geochim. Cosmochim. Acta 42, 495–506.

Espinasse, B., Hunt, B.P.V., Batten, S.D., Pakhomov, E.A., 2020. Defining isoscapes in the Northeast Pacific as an index of ocean productivity. Glob. Ecol. Biogeogr. 29, 246–261.

Espinoza, P., Bertrand, A., Van Der Lingen, C.D., Garrido, S., Rojas de Mendiola, B., 2009. Diet of sardine (*Sardinops sagax*) in the northern humboldt current system and comparison with the diets of clupeoids in this and other eastern boundary upwelling systems. Prog. Oceanogr. 83, 242–250.

Flaherty, E.A., Ben-David, M., 2010. Overlap and partitioning of the ecological and isotopic niches. Oikos 119, 1409–1416.

Fox, D.L., Coe, W.R., 1943. Biology of the California sea-mussel (*Mytilus californianus*). J. Exp. Zool. 87, 59–72.

Frolov, S.A., Kudela, R.M., Bellingham, J.G., 2013. Monitoring of harmful algal blooms in the era of diminishing resources: a case study of the U.S. West Coast. Harmful Algae 21–22, 1–12.

Garrison, D.L., 1979. Monterey bay phytoplankton I. seasonal cycles of phytoplankton assemblages. J. Plankton Res. 1, 241–266.

Goericke, R., Fry, B., 1994. Variations in marine plankton d13C with latitude, temperature, and dissolved CO2 in the world ocean. Global Biogeochem. Cycles 8, 85–90.

Goldstein, T., Mazet, J.A.K., Zabka, T.S., Langlois, G., Colegrove, K.M., Silver, M., Bargu, S., Van Dolah, F., Leighfield, T., Conrad, P.A., Barakos, J., Williams, D.C., Dennison, S., Haulena, M., Gulland, F.M.D., 2008. Novel symptomatology and changing epidemiology of domoic acid toxicosis in California sea lions (*Zalophus californianus*): an increasing risk to marine mammal health. Proc. R. Soc. B Biol. Sci. 275, 267–276.

Gómez-Gutiérrez, J., Peterson, W.T., Miller, C.B., 2005. Cross-shelf life-stage segregation and community structure of the euphausiids off central Oregon (1970-1972). Deep. Res. Part II Top. Stud. Oceanogr. 52, 289–315.

Graham, W.M., Largier, J.L., 1997. Upwelling shadows as nearshore retention sites: the example of northern monterey bay. Cont. Shelf Res. 17, 509–532.

Greig, D.J., Gulland, F.M.D., Kreuder, C., 2005. A decade of live California sea lion (*Zalophus californianus*) strandings along the central California coast: causes and trends, 1991-2000. Aquat. Mamm. 31, 11–22.

Gulland, F.M.D., 2000. Domoic acid toxicity in California sea lions (*Zalophus californianus*) stranded along the central California coast, May-October 1998. NOAA Technical Memorandum NMFS.

Gulland, F.M.D., Haulena, M., Fauquier, D., Langlois, G.W., Lander, M.E., Zabka, T., Duerr, R., 2002. Domoic acid toxicity in Californian sea lions: clinical signs, treatment and survival. Vet. Rec. 150, 475–480.
Harvey, C., Garfield, N., Williams, G., Tolimieri, N., Schroeder, I., Andrews, K., Barnas, K., Bjorkstedt, E., Bograd, S., Brodeur, R., Burke, B., Cope, J., Coyne, A., DeWitt, L., Dowell, J., Field, J., Fisher, J., Frey, P., Good, T., Greene, C., Hazen, E., Holland, D., Hunter, M., Jacobson, K., Jacox, M., Juhasz, C., Kaplan, I., Kasperski, S., Lawson, D., Leising, A., Manderson, A., Melin, S., Moore, S., Morgan, C., Muhling, B., Munsch, S., Norman, K., Robertson, R., Rogers-Bennett, L., Sakuma, K., Samhouri, J., Selden, R., Siedlecki, S., Somers, K., Sydeman, W., Thompson, A., Thorson, J., Tommasi, D., Trainer, V., Varney, A., Wells, B., Whitmire, C., Williams, M., Williams, T., Zamon, J., Zeman, S., 2019. Ecosystem status report of the California current for 2019: a summary of ecosystem indicators compiled by the California current integrated ecosystem assessment team (CCIEA). NOAA Technical Memorandum NMFS-NWFSC.
Holland, D.S., Leonard, J., 2020. Is a delay a disaster? economic impacts of the delay of the california dungeness crab fishery due to a harmful algal bloom. Harmful Algae 98.
Horner, R.A., Garrison, D.L., Plumley, F.G., 1997. Harmful algal blooms and red tide problems on the U.S. west coast. Limnol. Oceanogr 42, 1076–1088.
Hyslop, E.J., 1980. Stomach contents analysis—A review of methods and their application. J. Fish Biol. 17, 411–429.
Ish, T., Dick, E.J., Switzer, P.V., Mangel, M., 2004. Environment, krill and squid in the Monterey Bay: from fisheries to life histories and back again. Deep. Res. II 51, 849–862.
Jackson, A.L., Inger, R., Parnell, A.C., Bearhop, S., 2011. Comparing isotopic niche widths among and within communities: SIBER - stable isotope bayesian ellipses in R. J. Anim. Ecol. 80, 595–602.
Jackson, A.L., Parnell, A.C., 2020. Package 'SIBER.'.
Karpov, K.A., Cailliet, G.M., 1979. Prey composition of the market squid, Loligo opalescens berry, in relation to depth and location of capture, size of squid, and sex of spawning squid. Calif. Coop. Ocean. Fish. Investig. Rep.
Koehn, L.E., Essington, T.E., Marshall, K.N., Kaplan, I.C., Sydeman, W.J., Szoboszlai, A.I., Thayer, J.A., 2016. Developing a high taxonomic resolution food web model to assess the functional role of forage fish in the California Current ecosystem. Ecol. Modell. 335, 87–100.
Kudela, R.M., Frolov, S.A., Anderson, C.R., Bellingham, J.G., 2012. Leveraging ocean observatories to monitor and forecast harmful algal blooms: a case sudy of the U.S. West Coast.
Lane, J.Q., Raimondi, P.T., Kudela, R.M., 2009. Development of a logistic regression model for the prediction of toxigenic Pseudo-nitzschia blooms in Monterey Bay, California. Mar. Ecol. Prog. Ser. 383, 37–51.
Layman, C.A., Arrington, D.A., Montana, C.G., Post, D.M., 2007. Can stable isotope ratios provide for community-wide measures of trophic structure? Ecology 88, 42–48.
Lecher, A.L., Mackey, K., Kudela, R., Ryan, J., Fisher, A., Murray, J., Paytan, A., 2015. Nutrient loading through submarine groundwater discharge and phytoplankton growth in Monterey Bay. CA. Environ. Sci. Technol. 49, 6665–6673.
Lefebvre, K.A., Bargu, S., Kieckhefer, T., Silver, M.W., 2002a. From sanddabs to blue whales: the pervasiveness of domoic acid. Toxicon 40, 971–977.
Lefebvre, K.A., Powell, C.L., Busman, M., Doucette, G.J., Moeller, P.D.R., Silver, J.B., Miller, P.E., Hughes, M.P., Singaram, S., Silver, M.W., Tjeerdema, R.S., 1999. Detection of domoic acid in northern anchovies and California sea lions associated with an unusual mortality event. Nat. Toxins 7, 85–92.
Lefebvre, K.A., Silver, M.W., Coale, S.L., Tjeerdema, R.S., 2002b. Domoic acid in planktivorous fish in relation to toxic Pseudo-nitzschia cell densities. Mar. Biol. 140, 625–631.
Lefebvre, K.A., Robertson, A., 2010. Domoic acid and human exposure risks: a review. Toxicon 56, 218–230.
Lewitus, A.J., Horner, R.A., Caron, D.A., Garcia-Mendoza, E., Hickey, B.M., Hunter, M., Huppert, D.D., Kudela, R.M., Langlois, G.W., Largier, J.L., Lessard, E.J., RaLonde, R., Rensel, J.J.E., Strutton, P.G., Trainer, V.L., Tweddle, J.F., 2012. Harmful algal blooms along the North American west coast region: history, trends, causes, and impacts. Harmful Algae 19, 133–159.
Liu, K., Kaplan, I.R., 1989. The eastern tropical Pacific as a source of 15N-enriched nitrate in seawater off southern California. Limnol. Oceanogr. 34, 820–830.
Lowry, M., Stewart, B., Heath, C., Francis, J., 1991. Seasonal and annual variability in the diet of California sea lions Zolaphus californianus at San Nicolas Island, California, 1981-1986. US Fishery Bulletin 81, 331–336.
Madigan, D.J., Carlisle, A.B., Dewar, H., Snodgrass, O.E., Litvin, S.Y., Micheli, F., Block, B.A., 2012. Stable isotope analysis challenges wasp-waist food web assumptions in an upwelling pelagic ecosystem. Sci. Rep. 2, 1–10.
McCabe, R.M., Hickey, B.M., Kudela, R.M., Lefebvre, K.A., Adams, N.G., Bill, B.D., Gulland, F.M.D., Thomson, R.E., Cochlan, W.P., Trainer, V.L., 2016. An unprecedented coastwide toxic algal bloom linked to anomalous ocean conditions. Geophys. Res. Lett. 43, 10, 366-10,376.
McManus, M., Kudela, R., Silver, M., Steward, G., Donaghay, P., Sullivan, J., 2008. Cryptic blooms: are thin layers the missing connection? Estuaries and Coasts 31.
Mekebri, A., Blondina, G.J., Crane, D.B., 2009. Method validation of microcystins in water and tissue by enhanced liquid chromatography tandem mass spectrometry. J. Chromatogr. A 1216, 3147–3155.
Miller, T.W., Brodeur, R.D., 2007. Diets of and trophic relationships among dominant marine nekton within the northern California Current ecosystem. Fish. Bull. 105, 548–559.
Miller, T.W., Brodeur, R.D., Rau, G.H., Omori, K., 2010. Prey dominance shapes trophic structure of the northern California Current pelagic food web: Evidence from stable isotopes and diet analysis. Mar. Ecol. Prog. Ser. 420, 15–26.
Minagawa, M., Wada, E., 1984. Stepwise enrichment of 15 N along food chains: further evidence and the relation between δ15N and animal age. Geochim. Cosmochim. Acta 48, 1135–1140.
Newsome, S.D., Martinez del Rio, C., Bearhop, S., Phillips, D.L., 2007. A niche for isotopic ecology. Front. Ecol. Environ. 5, 429–436.
Newsome, S.D., Tinker, M.T., Monson, D.H., Oftedal, O.T., Ralls, K., Staedler, M.M., Fogel, M.L., Estes, J.A., 2009. Using stable isotopes to investigate individual diet specialization in California sea otters (*Enhydra lutris nereis*). Ecology 90, 961–974.
Paduan, J.D., Rosenfeld, L.K., 1996. Remotely sensed surface currents in monterey bay from shore-based HF radar (coastal ocean dynamics application radar). J. Geophys. Res. 101 (20), 669–686.
Peacock, M.B., Gibble, C.M., Senn, D.B., Cloern, J.E., Kudela, R.M., 2018. Blurred lines: multiple freshwater and marine algal toxins at the land-sea interface of San Francisco Bay, California. Harmful Algae 73, 138–147.
Peterson, B.J., Fry, B., 1987. Stable isotopes in ecosystem studies. Annu. Rev. Ecol. Evol. Syst. 18, 293–320.
Post, D.M., 2002. Using stable isotopes to estimate trophic position: models, methods, and assumptions. Ecology 83, 703–718.
Rau, G.H., Sweeney, R.E., Kaplan, I.R., 1982. Plankton 13C:12C ratio changes with latitude differences between northern and southern oceans. Deep Sea Res 29, 1035–1039.
Reilly, C.A., Echeverria, T.W., Ralston, S., 1992. Interannual variation and overlap in the diets of pelagic juvenile rockfish (Genus: *sebastes*) off central California. Fish. Bull. 90, 505–515.
Ritzman, J., Brodbeck, A., Brostrom, S., Mcgrew, S., Dreyer, S., Klinger, T., Moore, S.K., 2018. Economic and sociocultural impacts of fisheries closures in two fishing-dependent communities following the massive 2015 U.S. west coast harmful algal bloom. Harmful Algae 80, 35–45.
Rosenfeld, L.K., Schwing, F.B., Garfield, N., Tracy, D.E., 1994. Bifurcated flow from an upwelling center: a cold water source for Monterey Bay. Cont. Shelf Res. 14, 931–964.
Ruiz-Cooley, R.I., Engelhaupt, D.T., Ortega-Ortiz, J.G., 2012. Contrasting C and N isotope ratios from sperm whale skin and squid between the Gulf of Mexico and Gulf of California: effect of habitat. Mar. Biol. 159, 151–164.
Ruiz-Cooley, R.I., Gerrodette, T., 2012. Tracking large-scale latitudinal patterns of δ13C and δ15N along the E Pacific using epi-mesopelagic squid as indicators. Ecosphere 3.
Ryan, J.P., Chavez, F.P., Bellingham, J.G., 2005. Physical-biological coupling in Monterey Bay, California: topographic influences on phytoplankton ecology. Mar. Ecol. Prog. Ser. 287, 23–32.
Ryan, J.P., Greenfield, D., Marin, R., Preston, C., Roman, B., Jensen, S., Pargett, D., Birch, J.M., Mikulski, C.M., Doucette, G.J., Scholin, C.A., 2011. Harmful phytoplankton ecology studies using an autonomous molecular analytical and ocean observing network. Limnol. Oceanogr. 56, 1255–1272.
Ryan, J.P., Kudela, R.M., Birch, J.M., Blum, M., Bowers, H.A., Chavez, F.P., Doucette, G. J., Hayashi, K., Marin, R., Mikulski, C.M., Pennington, J.T., Scholin, C.A., Smith, G. J., Woods, A.L., Zhang, Y., 2017. Causality of an extreme harmful algal bloom in Monterey Bay, California, during the 2014-2016 northeast Pacific warm anomaly. Geophys. Res. Lett. 44, 5571–5579.
Ryan, J.P., McManus, M.A., Kudela, R.M., Artigas, M.L., Bellingham, J.G., Chavez, F.P., Doucette, G.J., Foley, D.G., Godin, M.A., Harvey, J.T., Marin, R., Messie, M., Mikulski, C.M., Pennington, T.J., Py, F., Rajan, K., Shulman, I., Wang, Z., Zhang, Y., 2014. Boundary influences on HAB phytoplankton ecology in a stratification-enhanced upwelling shadow. Deep. Res. II 101, 63–79.
Rykaczewski, R.R., Checkley, D.M., 2008. Influence of ocean winds on the pelagic ecosystem in upwelling regions. Proc. Natl. Acad. Sci. U. S. A. 105, 1965–1970.
Ryther, J.H., 1969. Photosynthesis and fish production in the sea. Science (80) 166, 72–76.
Saino, T., Hattori, A., 1980. 15 N natural abundance in oceanic suspended particulate matter. Nature 283, 752–754.
Sakuma, K., Field, J.C., Mantua, N., Marinovic, B., Carrion, C., 2016. Anomalous epipelagic micronekton assemblage patterns in neritic waters of the California Current in Spring 2015 during a period of extreme ocean conditions. Calif. Coop. Ocean. Fish. Invest. Rep. 57, 163–183.
Scholin, C.A., Gulland, F.M.D., Doucette, G.J., Benson, S., Busman, M., Chavez, F.P., Cordaro, J., DeLong, R., De Vogelaere, A., Harvey, J.T., Haulena, M., Lefebvre, K.A., Lipscomb, T., Losctutoff, S., Lowenstine, L., Marin, R., Miller, P.E., McLellan, W.A., Moeller, P.D.R., Powell, C.L., Rowles, T.K., Silvagni, P., Silver, M.W., Spraker, T., Trainer, V.L., Van Dolah, F.M., 2000. Mortality of sea lions along the central California coast linked to a toxic diatom bloom. Lett. to Nat. 403, 80–84.
Sekula-Wood, E., Schnetzer, A., Benitez-Nelson, C.R., Anderson, C.R., Berelson, W.M., Brzezinski, M.A., Burns, J.M., Caron, D.A., Cetinic, I., Ferry, J.L., Fitzpatrick, E., Jones, B.H., Miller, P.E., Morton, S.L., Schaffner, R.A., Siegel, D.A., Thunell, R., 2009. Rapid downward transport of the neurotoxin domoic acid in coastal waters. Nat. Geosci. 2, 272–275.
Smith, B.N., Epstein, S., 1971. Two categories of 13C/12C ratios for higher plants. Plant Physiol. 47, 380–384.
Smith, J., Connell, P., Evans, R.H., Gellene, A.G., Howard, M.D.A., Jones, B.H., Kaveggia, S., Palmer, L., Schnetzer, A., Seegers, B.N., Seubert, E.L., Tatters, A.O., Caron, D.A., 2018. A decade and a half of *Pseudo-nitzschia* spp. and domoic acid along the coast of southern California. Harmful Algae 79, 87–104.
Somes, C.J., Schmittner, A., Galbraith, E.D., Lehmann, M.F., Altabet, M.A., Montoya, J. P., Letelier, R.M., Mix, A.C., Bourbonnais, A., Eby, M., 2010. Simulating the global distribution of nitrogen isotopes in the. ocean 24, 1–16.
Stevens, B., Armstrong, D., Cusimano, R., 1982. Feeding habits of the dungeness crab Cancer magister as determined by the index of relative importance. Mar. Biol. 72.

Sun, J., Hutchins, D.A., Feng, Y., Seubert, E.L., Caron, D.A., Fu, .F..-X., 2011. Effects of changing pCO2 and phosphate availability on domoic acid production and physiology of the marine harmful bloom diatom *Pseudo-nitzschia multiseries*. Limnol. Oceanogr. 56, 829–840. https://doi.org/10.4319/lo.2011.56.3.0829.

Szoboszlai, A.I., Thayer, J.A., Wood, S.A., Sydeman, W.J., Koehn, L.E., 2015. Forage species in predator diets: synthesis of data from the California Current. Ecol. Inform. 29, 45–56.

Thompson, A.R., Schroeder, I.D., Bograd, S.J., Hazen, E.L., Jacox, M.G., Leising, A.W., 2018. State of the California current 2017-18: still not quite normal in the north and getting interesting in the south. Calif. Coop. Ocean. Fish. Investig. Rep. 59.

Trainer, V.L., Bates, S.S., Lundholm, N., Thessen, A.E., Cochlan, W.P., Adams, N.G., Trick, C.G., 2012. *Pseudo-nitzschia* physiological ecology, phylogeny, toxicity, monitoring and impacts on ecosystem health. Harmful Algae 14, 271–300.

Trainer, V.L., Moore, S.K., Hallegraeff, G.M., Kudela, R.M., Clement, A., Mardones, J.I., Cochlan, W.P., 2020. Pelagic harmful algal blooms and climate change: lessons from nature's experiments with extremes. Harmful Algae 91.

Trainer, V.L., Nicolaus, A.G., Bill, B.D., Stehr, C.M., Wekell, J.C., Moeller, P.D.R., Busman, M., Woodruff, D., 2000. Domoic acid production near California coastal upwelling zones, June 1998. Limnol. Oceanogr. 45, 1818–1833.

Umhau, B.P., Benitez-Nelson, C.R., Anderson, C.R., McCabe, K., Burrell, C., 2018. A time series of water column distributions and sinking particle flux of Pseudo-nitzschia and domoic acid in the Santa Barbara Basin, California. Toxins (Basel) 10.

Van Der Lingen, C.D., 2002. Diet of sardine *Sardinops sagax* in the southern Benguela upwelling ecosystem. South African J. Mar. Sci. 24, 301–316.

Van Der Lingen, C.D., Bertrand, A., Bode, A., Brodeur, R.D., Cubillos, P.E., Friedland, K., Garrido, S., Irigoien, X., Miller, T.W., Mollmann, C., Rodriguez-Sanchez, R., Tanaka, H., Temming, A., 2009. Trophic dynamics. In: Checkley, D.M., Alheit, J., Oozeki, Y., Roy, C. (Eds.), Climate Change and Small Pelagic Fish. p., (Eds), p. 333.

Van Der Lingen, C.D., Hutchings, L., Field, J.G., 2006. Comparative trophodynamics of anchovy Engraulis encrasicolus and sardine *Sardinops sagax* in the southern Benguela: are species alternations between small pelagic fish trophodynamically mediated? African J. Mar. Sci. 28, 465–477.

Van Der Lingen, C.D., Hutchings, L., Lamont, T., Pitcher, G.C., 2016. Climate change, dinoflagellate blooms and sardine in the southern benguela current large marine ecosystem. Environ. Dev. 17, 230–243.

Vander Zanden, M.J., Clayton, M.K., Moody, E.K., Solomon, C.T., Weidel, B.C., 2015. Stable isotope turnover and half-life in animal tissues: a literature synthesis. PLoS ONE 10, 1–16.

Vigilant, V.L., Silver, M.W., 2007. Domoic acid in benthic flatfish on the continental shelf of Monterey Bay, California, USA. Mar. Biol. 151, 2053–2062.

Weise, M.J., Harvey, J.T., 2008. Temporal variability in ocean climate and California sea lion diet and biomass consumption: implications for fisheries management. Mar. Ecol. Prog. Ser. 373, 157–172.

Wilkerson, F.P., Dugdale, R.C., Kudela, R.M., Chavez, F.P, 2000. Biomass and productivity in Monterey Bay, California: contribution of the large phytoplankton. Deep Sea Res. II 47, 1003–1022.

Wohlgeschaffen, G.D., Mann, K.H., Rao, Subba, D, V., Pocklington, R., 1992. Dynamics of the phycotoxin domoic acid: accumulation and excretion in two commercially important bivalves. J. Appl. Phycol. 4, 297–310.

Work, T.M., Barr, B., Beale, A.M., Fritz, L., Michael, A., Wright, J.L.C., Url, S., 1993. Epidemiology of domoic acid poisoning in brown pelicans (pelecanus occidentalis) and brandt's cormorants (*phalacrocorax penicillatus*) in California. J. Zoo Wildl. Med.

Zwolinski, J.P., Demer, D.A., Byers, K.A., Cutter, G.R., Renfree, J.S., Sessions, T.S., Macewicz, B.J., 2012. Distributions and abundances of pacific sardine (*Sardinops sagax*) and other pelagic fishes in the California current ecosystem during spring 2006, 2008, and 2010, estimated from acoustic-trawl surveys. Fish. Bull. 110, 110–122.

Further reading

McConnaughey, T., McRoy, C.P., 1979. Food-web structure and the fractionation of carbon isotopes in the Bering Sea. Mar. Biol. 262, 257–262.

Murry, B.A., Farrell, J.M., Teece, M.A., Smyntek, P.M., 2006. Effect of lipid extraction on the interpretation of fish community trophic relationships determined by stable carbon and nitrogen isotopes. Can. J. Fish. Aquat. Sci. 63, 2167–2172.